IEEE Access
Multidisciplinary | Rapid Review | Open Access Journal

Received March 2, 2021, accepted March 25, 2021, date of publication March 29, 2021, date of current version April 8, 2021.

Digital Object Identifier 10.1109/ACCESS.2021.3069469

SINS/DVL Integrated System With Current and Misalignment Estimation for Midwater Navigation

XIANJUN LIU[1,2], XIXIANG LIU[1,2], LEI WANG[3], YONGJIANG HUANG[1,2], AND ZIXUAN WANG[1,2]

[1]School of Instrument Science and Engineering, Southeast University, Nanjing 210096, China
[2]Key Laboratory of Micro-Inertial Instrument and Advanced Navigation Technology, Ministry of Education, Nanjing 210096, China
[3]College of Optical Science and Engineering, Zhejiang University, Hangzhou 310027, China

Corresponding author: Xixiang Liu (scliuseu@163.com)

This work was supported in part by the National Natural Science Foundation of China under Grant 51979041 and Grant 61973079, and in part by the Ministry of Education and Equipment Pre-research Joint Foundation under Grant 6141A02011906.

ABSTRACT Motivated by the problem that water-track Doppler Velocity Log (DVL) cannot effectively suppress the error accumulation of strap-down inertial navigation system (SINS), this paper proposes a novel SINS/DVL integrated navigation algorithm for deep and long cruising range Human Occupied Vehicle (HOV). Such algorithm decomposes the navigation process into two tightly coupled working modes: alignment mode and navigation mode. In the alignment mode, HOV is controlled to perform horizontal circular motion for several minutes to realize Self-Aided SINS. Combining the precise navigation solutions provided by Self-Aided SINS and measurements from DVL with water track, recursive least square (RLS) algorithm is adopted to estimate heading misalignment angle between SINS and DVL and horizontal ocean current velocity. In the navigation mode, both horizontal ocean current velocity obtained in the alignment mode and DVL measurements are utilized to assist SINS, thus enabling SINS/DVL/Current integrated navigation. A square trajectory with a navigation-grade inertial measurement unit (IMU) is simulated to evaluate the proposed SINS/DVL integrated navigation algorithm. Simulation results show that the proposed SINS/DVL integrated navigation is capable of suppressing SINS error divergence effectively and efficiently. In addition, the feasibility and effectiveness of Self-Aided SINS based on horizontal circular motion is also verified by field test with real IMU data.

INDEX TERMS HOV, SINS, DVL, midwater navigation, self-aided SINS.

I. INTRODUCTION

Human Occupied Vehicle (HOV) has become an indispensable platform for deep-sea research and exploration, since it is the only equipment that can directly send scientists and researchers to such extreme depth to perform underwater missions [1]–[3]. Due to the restriction of energy and maneuverability, accurate navigation has become a crucial factor for HOV to enhance its safety, improve underwater operation efficiency and further discover the scientific value of filed collected samples and data [4]. With the development of underwater navigation sensor technologies and fusion algorithms, existing navigation techniques have enabled successful operations of modern deep HOV, which are previously considered infeasible or unrealistic [1], [4], [5].

However, accurate navigation and localization is still significantly challenging for deep-diving HOV, especially in midwater where both Global Positioning System (GPS) and Doppler Velocity Log (DVL) are unavailable. For underwater navigation, vehicle depth can be precisely and directly obtained by a hydrostatic pressure sensor, whereas horizontal XY navigation is more difficult to achieve due to fewer available sensors [6], [7]. In fact, inertial measurement unit (IMU) and acoustic positioning system (APS), include ultra-short baseline (USBL), long baseline (LBL) and single-beacon navigation are the only available sensors for XY navigation in midwater [6]. Moreover, the motivation of improving midwater navigation arises from tasks demand for HOV hovering

The associate editor coordinating the review of this manuscript and approving it for publication was Pietro Savazzi.

at a designated position in midwater or cruising with constant height above seabed [1].

As a self-contained and frameless system, strap-down inertial navigation system (SINS), composed of three gyroscopes, three accelerometers and micro-computers, has been widely used for underwater navigation with the advantages of high reliability, strong independence, providing high-update-frequency and comprehensive navigation messages, and so on [8]–[12]. Unfortunately, such integration-based navigation system suffers from accumulated errors over time if adding information from external references are unavailable. On the other hand, APS can provide geo-referenced positioning information, but exist the defects of harsher application conditions requiring pre-arranged dedicated acoustic infrastructure and/or surface vessels [9], [10]. In addition, APS usually suffers from multi-path effect of underwater sound transmission, whose accuracy is relative to target range [10].

As a relatively mature navigation solution, SINS/DVL integrated navigation is widely used for underwater navigation with the advantages of autonomy and high accuracy [13]. The fact that DVL measurements (velocity relative to water) cannot be directly used for navigation has promoted and stimulated the development of other velocity-assisted navigation technologies suitable for midwater navigation, mainly including ocean current estimation and finding complementary or alternative for DVL [7], [10]–[12]. Based on the common hypothesis that ocean currents keep constant, Literature [7] presented an ADCP-aided localization method, which requires further investigation to integrate with INS. Literature [11] proposed a model-aided INS navigation scheme, whose performance is related to the accuracy of real-time ocean current estimation and kinematic vehicle model. By utilizing ADCP measurements and ocean current predictions provided by preloaded ocean current maps, Literature [12] proposed a current-aided inertial navigation framework. Despite significant effort and improvement, there are certain prerequisites or limitations for such technologies when applied in midwater operations.

Compared with SINS/USBL integrated navigation, which is an effective and widely applied solution for midwater navigation, SINS/DVL integrated navigation has the advantages of greater autonomy and lower cost. In view of this, a novel SINS/DVL integrated navigation system is designed for midwater navigation, which includes two working modes: alignment mode and navigation mode. In the alignment mode, it takes several minutes to estimate ocean current velocity and misalignments between SINS and DVL, which are the premise and basis of subsequent navigation mode. In the navigation mode, DVL measurements and ocean current velocity are utilized to assist SINS to restrain its error growth. The novel contributions of this work are as follows:

1) Estimating ocean current velocity and misalignment angle between SINS and DVL in the alignment mode.

2) Utilizing DVL measurements and ocean current to assist SINS in the navigation mode.

In what follows, problem analysis of SINS/DVL integrated navigation is introduced in Section II. Section III illustrates the Self-Aided SINS scheme includes introducing the mechanization and error model of SINS, discussing the design of IIR digital High-pass filter (HPF), and presenting kalman filter (KF) design. Current velocity and misalignment estimation is presented in Section IV. SINS/DVL/Current integrated navigation system is introduced in Section V. Simulations and Field test are shown in Section VI and VII, respectively. And conclusions are drawn in Section VIII.

II. PROBLEM ANALYSIS OF SINS/DVL INTEGRATED NAVIGATION

SINS/DVL integrated navigation system is commonly used for long-range underwater navigation, only requiring on-boad navigation sensors. DVL is an instrument that measures the velocity of underwater vehicle based on Doppler effect and usually has two working modes: bottom tracking mode and water tracking mode [14]–[16], which is used to restrain the error accumulation of SINS. For common underwater applications, DVL is working in bottom tracking mode, and the accuracy of SINS/DVL integrated navigation mainly depends on two factors: the scale factor of DVL and misalignments between SINS and DVL.

However, as to those underwater vehicles in midwater, DVL is working in water tracking mode, whose observations are unavailable to effectively suppress the error accumulation of SINS. As shown in Fig.1, the distance between ultrasonic transducer, installed at the bottom of underwater vehicle, and seabed exceeds the maximum range of DVL measurement. In such cases, DVL loses bottom tracking and can only work in water tracking mode to measure the velocity relative to set flow layer. For midwater navigation, the ground velocity of underwater vehicle should be obtained to effectively suppress the error accumulation of SINS, which is equal to DVL measurement plus ocean current velocity.

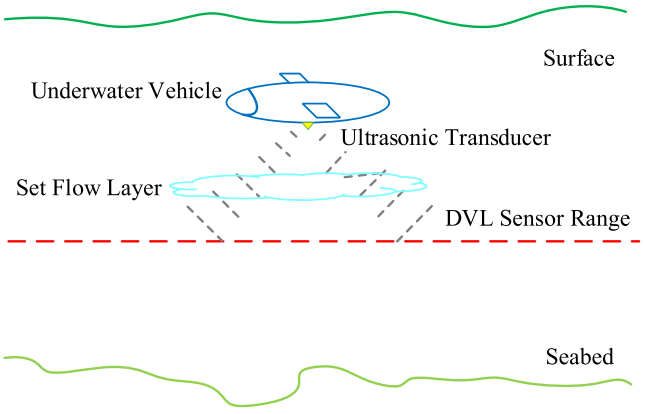

FIGURE 1. Diagrammatic sketch of DVL water tracking mode.

Based on the above analysis, in order to successfully implement SINS/DVL integrated navigation in midwater, it is necessary to obtain ocean current velocity in advance if it cannot be directly measured or estimated in-situ. According to the

existing ocean model, current velocity usually changes slowly in a small range, so it can be assumed that current velocity in a local sea with constant depth remains unchanged in the short term. Benefiting from the development of maneuvering control technology, steady-state maneuvering characteristics of underwater vehicle may make it possible for us to avoid the barriers of existing underwater navigation sensor technology and find a feasible midwater navigation scheme [17]–[19].

To this end, this paper proposes a novel SINS/DVL integrated navigation scheme for HOV operated in midwater as shown in Fig.2, which includes two tightly coupled working modes: alignment mode and navigation mode. In the alignment mode, HOV is controlled to execute a specific trajectory so as to realize Self-Aided SINS [20], which is based on error propagation of SINS and maneuvering characteristics of vehicle. Combined with DVL measurements (working in water tracking mode) and precise navigation solution of Self-Aided SINS, local ocean current velocity can be estimated effectively and efficiently. By assuming that ocean currents in a small range are constant within a short period of time, estimated ocean currents and DVL measurements are utilized to assist SINS, thus enabling the proposed SINS/DVL integrated navigation in the navigation mode. Different from traditional SINS/DVL integrated navigation, the accuracy of the proposed SINS/DVL integrated navigation mainly depends on three factors: the scale factor of DVL, misalignment between SINS and DVL, as well as ocean current. Moreover, the first factor is considered in the navigation mode, and the next two factors are treated in the alignment mode.

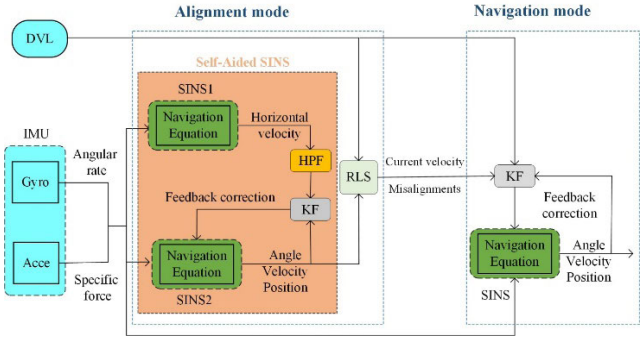

FIGURE 2. Illustration of SINS/DVL integrated navigation in midwater.

III. SELF-AIDED SINS BASED ON TRAJECTORY CONSTRAINTS

In order to estimate ocean current and misalignment between SINS and DVL effectively and efficiently, Self-Aided SINS algorithm should be realized to obtain precise navigation solutions in the alignment mode. Figure 2 illustrates the detailed realization of Self-Aided SINS scheme. When a HOV performs pre-defined maneuvering, the IMU data are took as system inputs to calculate the navigation equation twice in parallel, thereby obtaining two sets of mathematical SINS: SINS1 and SINS2. Considering that SINS horizontal velocity contains high-frequency true velocity based on trajectory constraints and low-frequency velocity error based on working mechanism of SINS, a delay correction-high-pass filter (DC-HPF) will be designed to handle horizontal velocity of SINS1. Finally, conventional KF technology is utilized to integrate obtained high-frequency true velocity with SINS2 to obtain navigation results without drift error, thus realizing the so-called Self-Aided SINS navigation scheme without requiring other external auxiliary navigation sensors [20].

A. MECHANISM AND ERROR MODEL OF SINS

Without loss of generality, the local geographical frame n (North-East-Downward) is selected as the navigation reference frame. Denote by b the SINS body frame aligned with the IMU axes, by e the Earth frame and by i Earth-centered initially-fixed orthogonal reference frame. The navigation solution of SINS can be calculated by three differential equations as follows [8]:

$$\dot{\boldsymbol{C}}_b^n = \boldsymbol{C}_b^n \left(\boldsymbol{\omega}_{nb}^b \times\right) \tag{1}$$

$$\dot{\boldsymbol{V}}^n = \boldsymbol{C}_b^n \boldsymbol{f}^b - \left(2\boldsymbol{\omega}_{ie}^n + \boldsymbol{\omega}_{en}^n\right) \times \boldsymbol{V}^n + \boldsymbol{g}^n \tag{2}$$

$$\dot{L} = \frac{V_N}{R_n + h}, \dot{\lambda} = \frac{V_E \sec L}{R_e + h}, \dot{h} = -V_D. \tag{3}$$

where $\boldsymbol{C}_b^n$ is the attitude matrix from the body frame to the local geographic frame, whose transposed matrix is $\boldsymbol{C}_n^b$; $\boldsymbol{\omega}_{nb}^b$ is angular rate of the body frame with respect to the navigation frame, expressed in the body frame, and the 3×3 skew symmetric matrix $(\cdot\times)$ is defined so that the cross product satisfies $\boldsymbol{a} \times \boldsymbol{b} = (\boldsymbol{a}\times)\boldsymbol{b}$ for arbitrary two vectors; $\boldsymbol{\omega}_{ie}^n$ is the Earth rotation rate with Ω denoting the Earth rate, and $\boldsymbol{\omega}_{en}^n$ is angular rate of the navigation frame with respect to the Earth frame; $\boldsymbol{\omega}_{ib}^b$ and $\boldsymbol{f}^b$ are the measurements of three orthogonally installed gyroscopes and three orthogonally installed accelerometers, denoting the angular rate and specific force respectively; $\boldsymbol{V}^n \left[\begin{array}{ccc} V_N & V_E & V_D \end{array}\right]^T$ is the velocity in the navigation frame denoting the north, east and downward velocities, respectively; The position $\boldsymbol{p} \left[\begin{array}{ccc} L & \lambda & h \end{array}\right]^T$ is commonly expressed as longitude, latitude and height above the Earth surface, which can be updated by the velocity where R_n and R_e are respectively the transverse and meridian radii of curvature, respectively.

Due to the existence of initial, sensors and navigation algorithm errors, the errors, defined as the difference between the calculated and true values, inevitably exist in attitude, velocity and position calculated by (1)-(3). Then the error propagation equations of SINS can be derived by perturbation method as follows:

$$\dot{\boldsymbol{\phi}}^n = -\boldsymbol{\omega}_{in}^n \times \boldsymbol{\phi}^n + \delta\boldsymbol{\omega}_{in}^n - \boldsymbol{C}_b^n \delta\boldsymbol{\omega}_{ib}^b \tag{4}$$

$$\begin{aligned} \delta\dot{\boldsymbol{V}}^n = &\left(\boldsymbol{C}_b^n \boldsymbol{f}^b\right) \times \boldsymbol{\phi}^n - \left(2\boldsymbol{\omega}_{ie}^n + \boldsymbol{\omega}_{en}^n\right) \times \delta\boldsymbol{V}^n \\ &- \left(2\delta\boldsymbol{\omega}_{ie}^n + \delta\boldsymbol{\omega}_{en}^n\right) \times \boldsymbol{V}^n + \boldsymbol{C}_b^n \delta\boldsymbol{f}^b \end{aligned} \tag{5}$$

$$\delta\dot{L} = \frac{1}{R_n + h}\delta V_N - \frac{V_N}{(R_e + h)^2}\delta h$$

$$\begin{aligned}\delta\dot{\lambda} &= \frac{1}{(R_e+h)\cos L}\delta V_E - \frac{\sin L}{(R_e+h)\cos^2 L}\delta L \\ &\quad - \frac{V_E}{(R_e+h)^2\cos L}\delta h \\ \delta\dot{h} &= -\delta V_D. \end{aligned} \tag{6}$$

where $\boldsymbol{\phi}^n = \begin{bmatrix}\phi_N & \phi_E & \phi_D\end{bmatrix}^T$ is attitude error vector describing the rotation between calculated and real navigation frame; $\delta \boldsymbol{V}^n \begin{bmatrix}\delta V_N & \delta V_E & \delta V_D\end{bmatrix}^T$ is velocity error vector; $\delta \boldsymbol{p} \begin{bmatrix}\delta L & \delta\lambda & \delta h\end{bmatrix}^T$ is position error vector, which denotes latitude error, longitude error and altitude error, respectively; $\delta\boldsymbol{\omega}_{ib}^b$ is the gyroscope error, and $\delta \boldsymbol{f}^b$ is the accelerometer error.

The precision of the SINS is mainly determined by the errors of inertial sensors, which is generally represented as a combination of random bias and random noise. In engineering, the one-order (or high-order) Markov process and white noise are applied to propagate random noise. In this paper, the main target is to deal with the Self-Aided SINS scheme so that the errors of IMU are assumed to be random walk bias error and white Gaussian noise. Thus, the error propagation models of gyroscopes and accelerometers can be constructed as follows [9], [21], [22]:

$$\delta\boldsymbol{\omega}_{ib}^b = \boldsymbol{\varepsilon}^b + \boldsymbol{w}_g,\ \dot{\boldsymbol{\varepsilon}}^b = 0,\ \boldsymbol{w}_g \sim N\left(0, \boldsymbol{Q}_g\right) \tag{7}$$

$$\delta \boldsymbol{f}^b = \boldsymbol{\nabla}^b + \boldsymbol{w}_a,\ \dot{\boldsymbol{\nabla}}^b = 0,\ \boldsymbol{w}_a \sim N\left(0, \boldsymbol{Q}_a\right). \tag{8}$$

where $\boldsymbol{\varepsilon}^b$ and $\boldsymbol{\nabla}^b$ are the constant errors of gyroscopes and accelerometers, respectively; $\boldsymbol{w}_g$ and $\boldsymbol{w}_a$ are the random errors of gyroscopes and accelerometers, respectively; $\boldsymbol{Q}_g$ and $\boldsymbol{Q}_a$ are the variance matrices of white noise corresponding to $\boldsymbol{w}_g$ and $\boldsymbol{w}_a$, respectively.

B. DC-HPF DESIGN

For underwater navigation, depth or height information can be precisely and directly obtained by a deep sensor, so the problem of horizontal XY navigation becomes the main object. For horizontal velocity outputs of SINS, there are:

$$\tilde{V}_N = V_N + \delta V_N \tag{9}$$

$$\tilde{V}_E = V_E + \delta V_E. \tag{10}$$

According to the error analysis of SINS in Section A, horizontal velocity errors $(\delta V_N, \delta V_E)$ include three kinds of different cycles of persistent oscillation, namely Schuler oscillation period T_s, earth oscillation period T_e, and Foucault oscillation period T_f [23]:

$$\begin{cases} T_s = 2\pi\sqrt{\dfrac{R}{g}} = 84.4\,\text{min} \\ T_e = \dfrac{2\pi}{\Omega} = 24h \\ T_f = \dfrac{2\pi}{\Omega\sin L}. \end{cases} \tag{11}$$

When HOV is controlled to perform periodic physical maneuvers, the true horizontal velocity (V_N, V_E), relative to the horizontal speed error $(\delta V_N, \delta V_E)$, can be regarded as high-frequency signals. That make it possible for extracting available auxiliary information from pure SINS output results to constitute self-assisted navigation system.

Maneuvering control technology is significant for underwater vehicles to operate tasks. Literature [17] proposed a mathematical model to verify the steady-state maneuvering characteristics of underwater vehicles, and used the test data collected by HUGIN 4000 AUV to evaluate the effectiveness of the algorithm. Square and turning maneuvers verification results indicate that the obtained parameters of the trajectories conform to physical interpretation. Literature [18] presented a cascade control method based on biological heuristics and sliding-mode control for the 7000-m "Jiaolong" HOV, which can achieve robust and accurate three-dimensional trajectory tracking. Literature [19] established a dynamic model of spiraling motion for underwater gliders assisted with Computational Fluid Dynamics (CFD) to obtain hydrodynamic coefficients. Based on previous analysis, it is entirely feasible for HOV to achieve steady-state maneuver characterizing constant depth and horizontal circle motion, which can be formulated as follows [18]:

$$\begin{cases} \gamma = 0 \\ \theta = 0 \\ \varphi = \omega_c t \end{cases} \tag{12}$$

$$\begin{cases} V_N = -r\omega_c\cos(\omega_c t) \\ V_E = r\omega_c\cos(\omega_c t) \\ V_D = 0 \end{cases} \tag{13}$$

where r denotes the radius of circular motion, $\omega_c = 2\pi/T_c$ denotes the angular rate of circular motion, T_c denotes the cycle of circular motion.

In fact, the order of the Infinite Impulse Response (IIR) filter is generally less than the Finite Impulse Response (FIR) filter under the same technical requirements, which means lower group delay, so IIR filter is chosen for real-time extraction of real horizontal velocity. Although a digital IIR HPF can be designed easily and suitably by using frequency transformation or analog to digital mapping technique, such traditional high-pass filter (T-HPF) exists the defects of phase shift and amplitude attenuation, and the error caused by phase shift is much larger than amplitude attenuation at the same time. In order to effectively solve the problem of signal delay, Literature [24] designed a zero-delay high-pass digital filter (ZD-HPF) to obtain ship's heave motion parameters based on so-called complementary technology. ZD-HPF can solve the problem of phase shift effectively and efficiently, but will cause greater amplitude attenuation compared to T-HPF.

To this end, this paper proposed a delay-correction high-pass filter (DC-HPF) to deal with horizontal velocity provided by SINS, which can not only solve the problem of phase shift but also keep phase attenuation unchanged when compared to T-HPF. In fact, the leading phase-angle and time

of T-HPF can be rigorously calculated by:

$$\begin{cases} \theta(\bar{\omega}) = \arg H\left(\exp(j\bar{\omega}T_{sp})\right) \\ t(\bar{\omega}) = \dfrac{\theta(\bar{\omega})}{\bar{\omega}} \end{cases} \tag{14}$$

where $H(\cdot)$ denotes transfer function of digital filter; $\bar{\omega}$ denotes angular rate of input signal; T_{sp} is sampling period, which is equal to navigation solution period here. In addition, robust control algorithm will be designed for spiral-diving HOV to keep its maneuvering in accordance with the pre-designed trajectory as much as possible. In view of this, we can obtain the value of angular rate of input signal in advance with $\bar{\omega} \approx \omega_c$. Thus, we can obtain the leading time between output signals processed by T-HPF and real signals. Then N-bit delay buffer should be set up in the computer to delay the output of T-HPF accordingly and the value of N can be calculated by:

$$N = \frac{t(\bar{\omega})}{T_{sp}}. \tag{15}$$

In final, the detailed descriptions of delay correction High-pass filter (DC-HPF) are summarized as follows:

1) Designing reasonable IIR digital high-pass filter specifications (f_p, f_s, A_p, A_s) based on spectrum analysis and obtain transfer function of the digital filter $H(z)$;

2) Calculating the leading time $t(\bar{\omega})$ by Eq. (14) and the number of delay buffers N by Eq. (15);

3) Delaying the output of T-HPF for N bit.

C. VELOCITY-AIDED SINS

Then, KF is designed to fuse SINS with horizontal velocity obtained from DC-HPF. The 15-dimension state vector and 2-dimension measurement vector is defined respectively as follows:

$$\boldsymbol{X}_1 = \begin{bmatrix} (\boldsymbol{\phi}^n)^T & (\delta\boldsymbol{V}^n)^T & (\delta\boldsymbol{p})^T & \left(\boldsymbol{\varepsilon}^b\right)^T & \left(\boldsymbol{\nabla}^b\right)^T \end{bmatrix}^T \tag{16}$$

$$\boldsymbol{Z}_1 = \begin{bmatrix} \tilde{V}_N - \bar{V}_N & \tilde{V}_E - \bar{V}_E \end{bmatrix}^T \tag{17}$$

where $\bar{V}_N$ and $\bar{V}_E$ denote horizontal velocity obtained from DC-HPF.

The discrete process model and observation model are:

$$\begin{cases} \boldsymbol{X}_k = \boldsymbol{\phi}_{k,k-1}\boldsymbol{X}_{k-1} + \boldsymbol{\Gamma}_{k,k-1}\boldsymbol{W}_{k-1} \\ \boldsymbol{Z}_k = \boldsymbol{H}_k\boldsymbol{X}_k + \boldsymbol{V}_k \end{cases} \tag{18}$$

where the subscript k denotes the k-th time-step; $\boldsymbol{\phi}$ denotes the transition matrix of the dynamic model, which can be obtained according to SINS error model; $\boldsymbol{H}$ denotes the measurement model matrix; $\boldsymbol{\Gamma}$ denotes the system noise matrix; $\boldsymbol{W}$, $\boldsymbol{V}$ denotes the process noise and the measurement noise, respectively.

Given the initial value $\hat{\boldsymbol{X}}_0$ and $\boldsymbol{P}_0$, the state estimation $\hat{\boldsymbol{X}}_k$ can be recursively calculate with observation $\boldsymbol{Z}_k$ as follows:

$$\hat{\boldsymbol{X}}_{k,k-1} = \boldsymbol{\phi}_{k,k-1}\hat{\boldsymbol{X}}_{k-1} \tag{19}$$

$$\hat{\boldsymbol{X}}_k = \hat{\boldsymbol{X}}_{k,k-1} + \boldsymbol{K}_k\left[\boldsymbol{Z}_k - \boldsymbol{H}_k\hat{\boldsymbol{X}}_{k,k-1}\right] \tag{20}$$

$$\boldsymbol{K}_k = \boldsymbol{P}_{k,k-1}\boldsymbol{H}_k^T\left[\boldsymbol{H}_k\boldsymbol{P}_{k,k-1}\boldsymbol{H}_k^T + \boldsymbol{R}_k\right]^{-1} \tag{21}$$

$$\boldsymbol{P}_{k,k-1} = \boldsymbol{\phi}_{k,k-1}\boldsymbol{P}_{k-1}\boldsymbol{\phi}_{k,k-1}^T + \boldsymbol{\Gamma}_{k,k-1}\boldsymbol{Q}_{k-1}\boldsymbol{\Gamma}_{k,k-1}^T \tag{22}$$

$$\boldsymbol{P}_k = [\boldsymbol{I} - \boldsymbol{K}_k\boldsymbol{H}_k]\boldsymbol{P}_{k,k-1} \tag{23}$$

where $\hat{\boldsymbol{X}}$ is the estimation for state vector $\boldsymbol{X}$; $\boldsymbol{P}$ is the state variance; $\hat{\boldsymbol{X}}_{k,k-1}$ is the predicted state estimate, and $\boldsymbol{P}_{k,k-1}$ is the corresponding covariance; $\boldsymbol{K}$ is the gain matrix; and $\boldsymbol{I}$ is the unit matrix with corresponding dimensions.

IV. CURRENT VELOCITY AND MISALIGNMENT ESTIMATION

Usually, the real DVL measurements can be modeled as [16]:

$$\tilde{\boldsymbol{V}}^d = (1 + \delta k)\,\boldsymbol{V}^d + \delta\boldsymbol{V}^d. \tag{24}$$

where δk denotes DVL scale factor error with $\delta k = 0$, $\boldsymbol{V}^d$ is the ideal velocity relative to ocean current in the instrument frame of DVL (d-frame), $\delta\boldsymbol{V}^d$ denotes DVL measurement noise.

The relationship of related velocity can be formulated as follows:

$$\boldsymbol{V}^n = \boldsymbol{C}_b^n\boldsymbol{C}_d^b\tilde{\boldsymbol{V}}^d + \boldsymbol{V}_c^n \tag{25}$$

where $\boldsymbol{V}^n$ and $\boldsymbol{C}_b^n$ are velocity in n-frame and attitude matrix provided by Self-Aided SINS, respectively; $\boldsymbol{V}_c^n = \begin{bmatrix} V_{cN} & V_{cE} & V_{cD} \end{bmatrix}^T$ is the ocean current velocity in n-frame; $\boldsymbol{C}_d^b$ is the attitude transformation matrix from d-frame to b-frame, which can be calculated by:

$$\boldsymbol{C}_d^b = \boldsymbol{I} - (\boldsymbol{\alpha}\times) \tag{26}$$

where $\boldsymbol{\alpha} = \begin{bmatrix} \alpha_\gamma & \alpha_\theta & \alpha_\varphi \end{bmatrix}^T$ denotes misalignment angle between SINS and DVL with $\dot{\boldsymbol{\alpha}} = \boldsymbol{0}$; α_γ and α_θ are horizontal misalignment angle, and α_φ is heading misalignment angle.

Substituting equation (26) into equation (25) yields:

$$\boldsymbol{V}^n - \boldsymbol{C}_b^n\tilde{\boldsymbol{V}}^d = \boldsymbol{C}_b^n\left(\tilde{\boldsymbol{V}}^d\times\right)\boldsymbol{\alpha} + \boldsymbol{V}_c^n. \tag{27}$$

Usually, only the horizontal velocity needs to be considered for XY navigation. Here, the 5-dimension state vector and 2-dimension measurement vector is defined respectively as follows:

$$\boldsymbol{X}_2 = \begin{bmatrix} \alpha_\gamma & \alpha_\theta & \alpha_\varphi & V_{cN} & V_{cE} \end{bmatrix}^T \tag{28}$$

$$\boldsymbol{Z}_2 = \begin{bmatrix} Z_{a1} & Z_{a2} \end{bmatrix}^T \tag{29}$$

where $\boldsymbol{Z}_a = \boldsymbol{V}^n - \boldsymbol{C}_b^n\boldsymbol{V}''$. For constant identification, recursive least square (RLS) algorithm is adopted to estimate installation deviation angle and horizontal ocean current velocity.

As to horizontal circle motion, we have:

$$\boldsymbol{C}_b^n = \begin{bmatrix} \cos(\omega_c t) & -\sin(\omega_c t) & 0 \\ \sin(\omega_c t) & \cos(\omega_c t) & 0 \\ 0 & 0 & 1 \end{bmatrix}. \tag{30}$$

Substituting equation (30) into equation (27) yields, as well as organizing the terms yield:

$$\begin{cases} V_N - \cos(\omega_c t)\tilde{v}_x^d + \sin(\omega_c t)\tilde{v}_y^d \\ \quad = \left(\sin(\omega_c t)\tilde{v}_x^d + \cos(\omega_c t)\tilde{v}_y^d\right)\alpha_\varphi + V_{cN} \\ V_E - \sin(\omega_c t)\tilde{v}_x^d - \cos(\omega_c t)\tilde{v}_y^d \\ \quad = \left(-\cos(\omega_c t)\tilde{v}_x^d + \sin(\omega_c t)\tilde{v}_y^d\right)\alpha_\varphi + V_{cE}. \end{cases} \tag{31}$$

According to analytical method of observability analysis [25], α_φ, V_{cN} and V_{cE} can be calculated by (31) with time change (at least two timestamps), which means that they can be estimated effectively in the alignment mode; While α_γ and α_θ are not able to be obtained by (31), which means that they cannot be estimated.

V. SINS/DVL/CURRENT INTEGRATED NAVIGATION

According to existing ocean model, horizontal current velocity usually keeps constant in 1-2 hours. In the navigation mode, HOV is able to cruise in midwater due to available SINS/DVL integrated navigation. Considering that α_γ and α_θ are usually very little, and α_φ can be obtained in the first stage, so installation deviation angle is ignored in the navigation mode for convenience with $\boldsymbol{C}_d^b = \boldsymbol{I}$.

The ideal and actual velocity in n-frame related to DVL measurements is calculated respectively as follows:

$$\boldsymbol{V}_{DVL}^n = \boldsymbol{C}_b^n \boldsymbol{C}_d^b \boldsymbol{V}^d + \boldsymbol{V}_c^n = \boldsymbol{C}_b^n \boldsymbol{V}^d + \boldsymbol{V}_c^n \tag{32}$$

$$\tilde{\boldsymbol{V}}_{DVL}^n = \left[\boldsymbol{I} - (\boldsymbol{\phi}^n\times)\right]\boldsymbol{C}_b^n(1+\delta k)\,\boldsymbol{V}^d + \boldsymbol{V}_c^n + \delta\boldsymbol{V}. \tag{33}$$

where δV denotes measurement error, including DVL measurement error and ocean current estimation error.

Expanding (33) and ignoring the second-order small quantity, we can get velocity error in n-frame:

$$Z_b = \tilde{\boldsymbol{V}}_{SINS}^n - \tilde{\boldsymbol{V}}_{DVL}^n = -\left(\boldsymbol{C}_b^n \boldsymbol{V}^d\right)\times\boldsymbol{\phi}^n + \delta\boldsymbol{V}^n - \delta k \boldsymbol{C}_b^n \boldsymbol{V}^d - \delta\boldsymbol{V} \tag{34}$$

where $\boldsymbol{Z}_b = \left[Z_{b1}\ Z_{b2}\ Z_{b3}\right]^T$. A 16-dimension kalman filter (KF) is employed to fuse SINS with DVL. Here, the state vector $\boldsymbol{X}_3$ and measurement vector $\boldsymbol{Z}_3$ is respectively defined as:

$$\boldsymbol{X}_3 = \left[(\boldsymbol{\phi}^n)^T\ (\delta\boldsymbol{V}^n)^T\ (\delta\boldsymbol{p})^T\ \left(\boldsymbol{\varepsilon}^b\right)^T\ \left(\boldsymbol{\nabla}^b\right)^T\ \delta k\right]^T \tag{35}$$

$$\boldsymbol{Z}_3 = \left[Z_{b1}\quad Z_{b2}\right]^T. \tag{36}$$

VI. SIMULATIONS

A. SIMULATION SETTING

In order to verify the feasibility and effectiveness of the proposed SINS/DVL integrated navigation in midwater as shown in Fig.2, a simulation test was carried out. The cruise trajectory with constant depth is shown in Fig.3, including ten consecutive circular trajectories with a radius of 10m and a square trajectory with a side length of 1km, corresponding to alignment mode and navigation mode, respectively. The trajectory parameters of the starting point were set as: attitude $\left[0°\ 0°\ 90°\right]$, velocity $\left[0\ 2m/s\ 0\right]$ and position $\left[32°\ 118°\ -4000m\right]$.

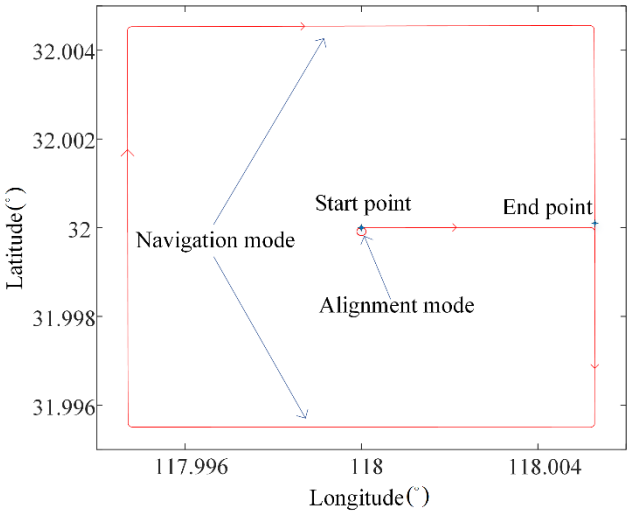

FIGURE 3. The ideal cruise trajectory of HOV in midwater.

Usually, the real IMU data is simulated by adding sensor error and ideal IMU data, which can be obtained by backsteping of navigation solution based on the set trajectory. Here, the gyro random biases were all set as $0.01°/h$ and random noises were white Gaussian noise with zero mean and standard deviation of $0.01°/h$ [21]. And the accelerometer random biases were all set as $50\mu g$ and random noises were white Gaussian noise with zero mean and standard deviation of $50\mu g$. The update frequencies of IMU data and SINS output data were both 100 Hz, while the update frequency of DVL was 1Hz. The scale factor error of DVL was set as 0.2%, and the ideal horizontal ocean current velocity was set as: $V_{cN} = 0.15m/s$ (North), $V_{cE} = 0.2m/s$ (East). To evaluate the effects of different schemes, the ideal trajectory and parameters were utilized as a reference.

B. SIMULATION RESULTS AND ANALYSES

In the alignment mode, HPF should be designed to deal with horizontal velocity provided be one SINS. Figure 4 shows the horizontal velocity error of the four different schemes, in which the red lines indicate the results of pure SINS, the green lines indicate the results of T-HPF, the blue lines indicate the results of ZD-HPF, and the lines indicate the results of DC-HP. As can be seen from Fig.4, horizontal velocity error of SINS diverges with time, which is accordance with theoretical analysis. Compared to T-HPF, horizontal velocity error of ZD-HPF and DC-HPF can both converge to the values near zero after 100s. Moreover, compared with ZD-HPF, DC-HPF has faster convergence and smaller distortion. In Table 1, it can be seen that the mean of ZD-HPF are bigger than T-HPF, while the standard deviation (Std) of ZD-HPF are smaller than T-HPF. This phenomenon is in accordance with the conclusion that ZD-HPF will cause greater amplitude attenuation when compared to T-HPF, while solving the problem of phase shift. The lines

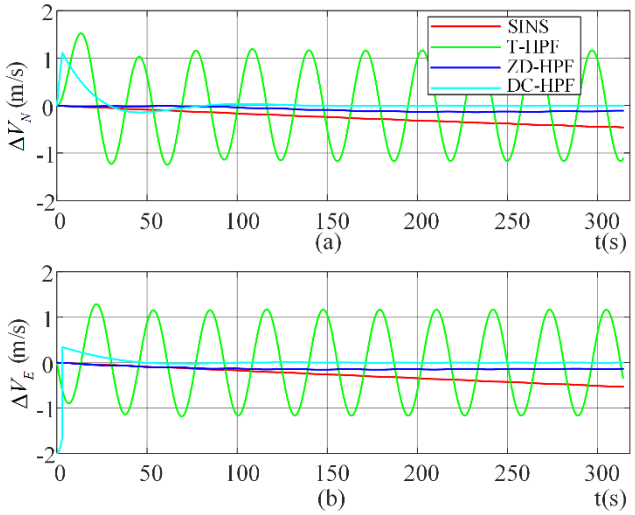

FIGURE 4. Horizontal velocity error among different schemes in the first stage.

TABLE 1. Statistical results of horizontal velocity error among different schemes in the first stage.

Statics	Mean		Std	
	ΔV_N (m/s)	ΔV_E (m/s)	ΔV_N (m/s)	ΔV_E (m/s)
SINS	-0.3201	-0.3551	0.0857	0.1043
T-HPF	0.0177	0.02	0.8284	0.8251
ZD-HPF	-0.1098	-0.1449	0.0264	0.0058
DC-HPF	0.0013	0.0006	0.0097	0.0022

in Fig.4 and statistics in Table 1 all indicate that DC-HPF outperforms both T-HPF and ZD-HPF.

In order to evaluate navigation performance of the proposed algorithm in the alignment mode, both the Reference system and the SINS system are compared with the Self-Aided SINS system. As the altitude information can be easily and precisely instrumented by a depth sensor, only horizontal velocity and position are involved to evaluate. Figures (5)-(7) show respectively the attitude, horizontal velocity and horizontal position among different schemes, in which the red lines indicate the navigation results of the SINS system, while the green and blue lines indicate the navigation solutions of the Reference and Self-Aided SINS system. It can be seen that the blue lines are extremely close to the green lines, while the red lines deviate from the green lines in Figs. (5)-(7). This phenomenon reveals the fact that pure SINS cannot be directly used for midwater navigation, while the proposed Self-Aided SINS system is effective and feasible. For Self-Aided SINS in Figs. (5)-(7), it starts to execute after 60 seconds due to the fact that the obtained horizontal velocities from DC-HPF converge when $t \geq 60s$ as shown in Fig.5. As can be seen from Fig. 6, the horizontal attitude (Roll and Pitch) curves converge to zero

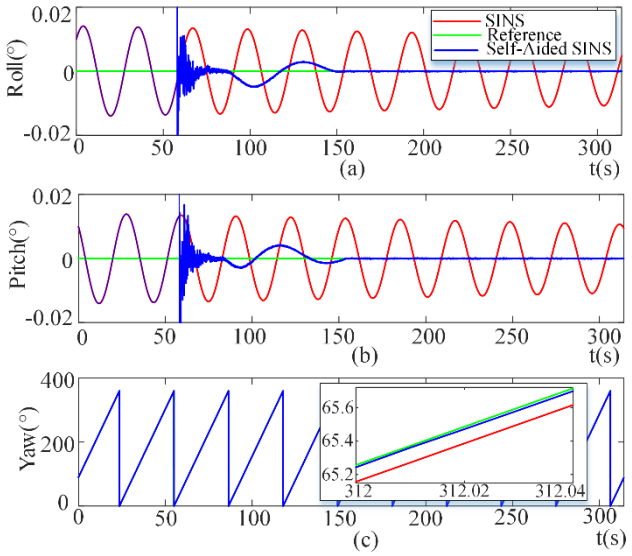

FIGURE 5. Attitude among different schemes in the first stage.

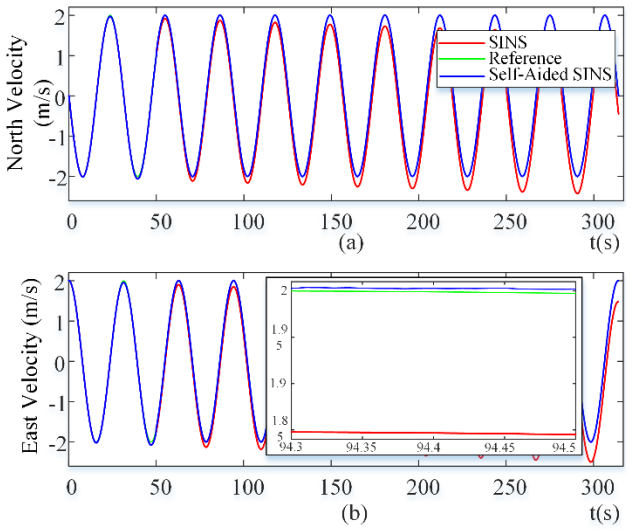

FIGURE 6. Horizontal velocity among different schemes in the first stage.

when $t \geq 150s$. Table 2 shows respectively the mean and standard over the last 150 seconds of attitude, horizontal velocity and horizontal position error from Self-Aided SINS. In order to further illustrate positioning performance in Fig.7, the errors of longitude and latitude in meters are chosen as performance metrics, which are defined as follows:

$$\begin{cases} \Delta x = \left(\bar{L} - L\right)\left(R_n + h\right) \\ \Delta y = \left(\bar{\lambda} - \lambda\right)\left(R_e + h\right)\cos L. \end{cases} \tag{37}$$

Both Figs. (5)-(7) and Table 2 indicate that Self-Aided SINS can provide precise navigation solution, whose error does not accumulate over time.

Figures 8 and 9 show the results of installation deviation angle and horizontal current velocity estimation by utilizing the obtained precise navigation solution from Self-Aided

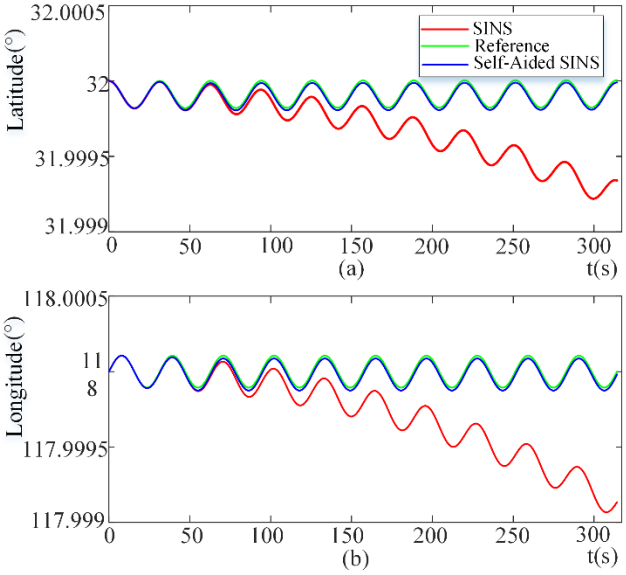

FIGURE 7. Horizontal position among different schemes in the first stage.

TABLE 2. Statistical results of navigation solution error for self-aided sins with $t = 150 - 314.16s$.

Statistics	Mean	Std
$\Delta\gamma(^\circ)$	-9.6650×10^{-7}	4.9031×10^{-5}
$\Delta\theta(^\circ)$	-1.1957×10^{-5}	9.5427×10^{-5}
$\Delta\varphi(^\circ)$	-0.0184	0.0221
$\Delta V_N(m/s)$	-0.0027	0.0044
$\Delta V_E(m/s)$	-1.1001×10^{-4}	0.0040
$\Delta x(m)$	-3.0820	0.1266
$\Delta y(m)$	-2.8682	0.0213

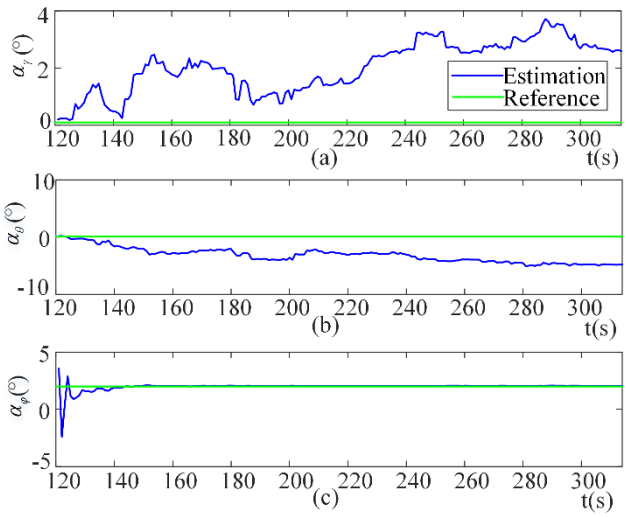

FIGURE 8. Estimation of installation deviation angle between SINS and DVL in the first stage.

SINS and DVL measurements with $t = 120 - 314s$. As can be seen from Figs. 8 and 9, the blue lines (denoting estimation) of horizontal installation deviation angle $(\alpha_\gamma, \alpha_\theta)$

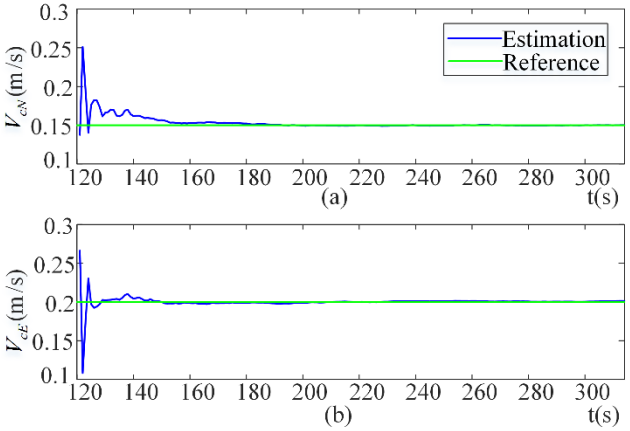

FIGURE 9. Estimation of horizontal ocean current velocity in the first stage.

deviate from the green lines (denoting the set reference value) while the blue lines of heading installation deviation angle (α_φ) and horizontal ocean current velocity (V_{cN}, V_{cE}) all converge near the green lines, which is consistent with the observability analysis in Section III. In order to further investigate the influence of different installation deviation angle on the estimation effect of α_φ, V_{cN} and V_{cE}, the statistics of their estimation error are given in three cases: $\alpha = \begin{bmatrix} 0.1^\circ & 0.1^\circ & 0.5^\circ \end{bmatrix}^T$ (Case 1), $\alpha = \begin{bmatrix} 0.01^\circ & 0.01^\circ & 0.1^\circ \end{bmatrix}^T$ (Case 2), $\alpha = \begin{bmatrix} 0.1^\circ & 0.1^\circ & 2^\circ \end{bmatrix}^T$ (Case 3). As can be concluded from Table 3, estimation errors of α_φ, V_{cN} and V_{cE} are almost the same under different installation deviation angle conditions.

TABLE 3. Statistical of estimation error among three cases.

Estimation error		Case 1	Case 2	Case 3
$\Delta\alpha_\varphi(^\circ)$	Mean	0.0645	0.0722	0.0575
	Std	0.0116	0.0121	0.0121
$\Delta V_{cN}(m/s)$	Mean	1.7678×10^{-4}	1.9312×10^{-4}	3.8988×10^{-4}
	Std	0.0012	0.0012	0.0012
$\Delta V_{cE}(m/s)$	Mean	-8.9632×10^{-5}	-1.9211×10^{-4}	5.2389×10^{-5}
	Std	9.6959×10^{-4}	9.2463×10^{-4}	0.0010

Figures (10)-(12) show the navigation solution of SINS/DVL in the second stage, in which the red lines indicate the navigation results of the SINS system, while the green and blue lines indicate the navigation solutions of the Reference and SINS/DVL system. Compared to SINS, the navigation results of SINS/DVL are closer to the ideal values, whose position error accumulate slowly over time. In the navigation mode, HOV travelled for 4.8 km and the accuracy of SINS/DVL is 0.08% (1σ) of distance travelled.

VII. FIELD TEST

The key of SINS/DVL integrated navigation in midwater lies in the Self-Aided SINS navigation based on horizontal

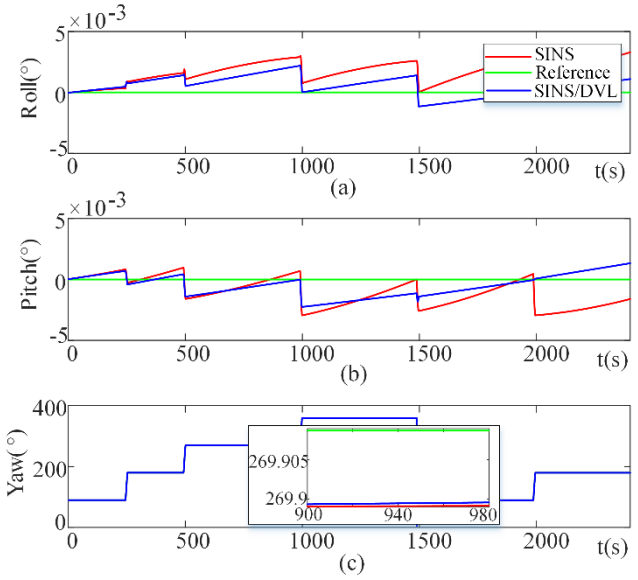

FIGURE 10. Attitude among different schemes in the second stage.

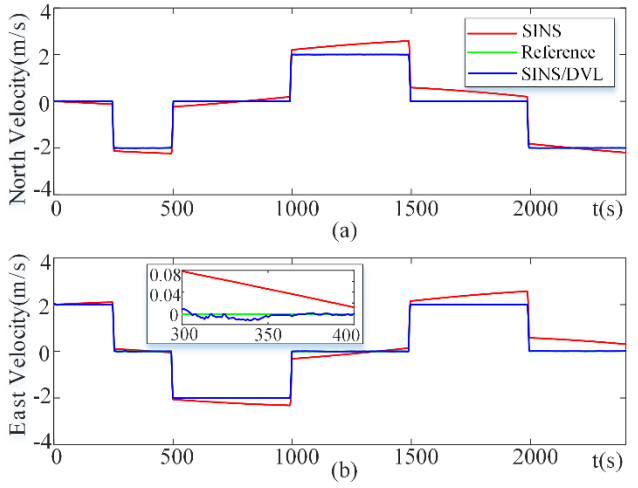

FIGURE 11. Horizontal velocity among different schemes in the second stage.

circular motion in the alignment mode, whose realization makes it possible to estimate horizontal ocean currents, and further realize SINS/DVL integrated navigation. In order to further verify the feasibility and effectiveness of the Self-Aided SINS navigation algorithm with real IMU data, a sports car test that simulates horizontal circular motion was carried out. The whole test lasts about 2 hours. A navigation-grade SINS which consisted of three fiber optic gyroscopes and three quartz accelerometers was installed in the trunk of the car, where the gyro bias was $0.01°/h$ and the accelerometer accuracy was $50\mu g$ with the GPS antenna installed on the top of the car, as show in Fig. 13.

SINS initial alignment was performed under static condition, including coarse alignment (10s) and fine alignment (110s). After 110s, SINS starts to enter the navigation mode,

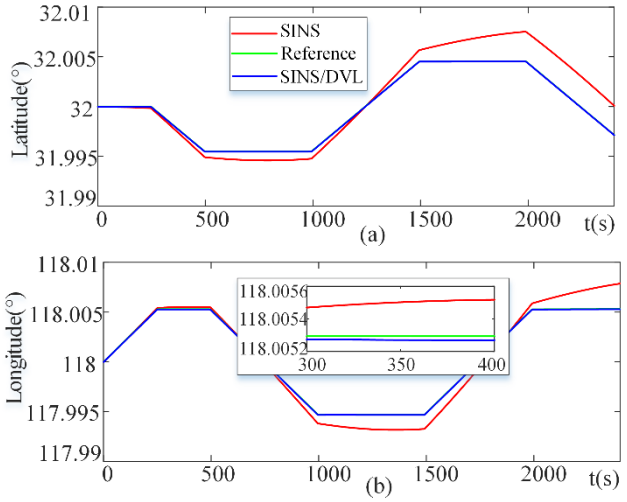

FIGURE 12. Horizontal position among different schemes in the second stage.

FIGURE 13. Equipment installation diagram in field test.

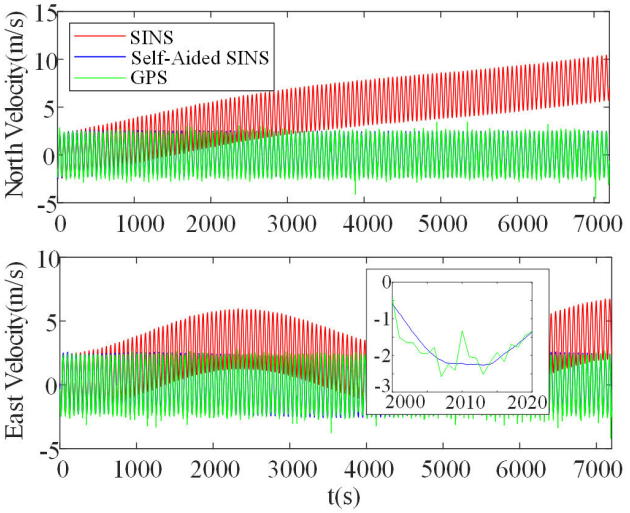

FIGURE 14. Comparison of horizontal velocity in field test.

and the initial attitude angle can be obtained by initial alignment with $\gamma = 2.41°$, $\theta = 0.58°$, and $\varphi = 80.21°$.

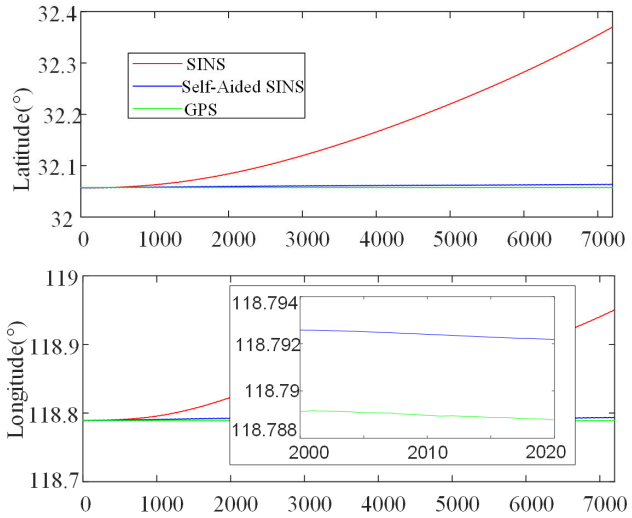

FIGURE 15. Comparison of horizontal position in field test.

In addition, the velocities at the initial moment are all as 0m/s, and the position are provided by GPS with $L = 32.05757459°, \lambda = 118.7889668°$, and $h = 14.45m$. When the vehicle moves in circles, it starts to perform Self-Aided SINS navigation algorithm whose results are shown in Figs. 14 and 15, in which the red lines indicate the navigation results of the SINS system, while the green and blue lines indicate the navigation solutions of GPS and Self-Aided SINS. It can be seen that the blue lines are extremely close to the green lines, while the red lines deviate from the green lines in Figs. 14 and 15. Such results verify the effectiveness and feasibility of Self-Aided SINS algorithm.

VIII. CONCLUSION

In this paper, we mainly focus on the problem of midwater navigation for HOV in the context of few sensors are available in midwater. In order to solving the problem that DVL is not directly available for midwater navigation and the drifts of SINS solutions are inevitable and accumulate over time, a novel SINS/DVL integrated navigation is proposed for HOV. For DVL working in the water tracking mode, in order to successfully implement SINS/DVL integrated navigation, ocean current velocity should be obtained in advance if it cannot be directly measured or estimated in-situ. To this end, the proposed algorithm decomposes the task into two tightly coupled working modes: alignment mode and navigation mode. In the alignment mode, Self-Aided SINS based on trajectory constraints is executed to provide precise navigation solutions for the estimation of horizontal ocean current velocity. After obtaining horizontal ocean current velocity, SINS/DVL integrated navigation can be established in the navigation mode.

To the best of our knowledge, this is the first effort to estimate ocean current only utilizing IMU and DVL in midwater. Simulation results verify the feasibility and effectiveness of the proposed SINS/DVL integrated navigation with the capability to suppress error divergence of SINS just like traditional SINS/DVL, whose positioning accuracy is 0.08% (1σ) of distance travelled. Meanwhile, the limitation and disadvantage of such scheme are that it requires specific maneuver for underwater vehicle and the accuracy is closely related to ocean current estimation. In addition, sports car test was carried out and experiment results have verified the feasibility and effectiveness of the Self-Aided SINS navigation based on horizontal circular motion with real IMU data.

ACKNOWLEDGMENT

The authors would like to thank Ms. Chen Xiaoshu for her work on language and grammar expression in this article.

REFERENCES

[1] F. Liu, W. Cui, and X. Li, "China's first deep manned submersible, JIAOLONG," *Sci. China Earth Sci.*, vol. 53, no. 10, pp. 1407–1410, Oct. 2010, doi: 10.1007/s11430-010-4100-2.

[2] N. Vedachalam, G. A. Ramadass, and M. A. Atmanand, "Reliability centered modeling for development of deep water human occupied vehicles," *Appl. Ocean Res.*, vol. 46, pp. 131–143, Jun. 2014, doi: 10.1016/j.apor.2014.03.001.

[3] E. Bergman, "Manned submersibles translating the ocean sciences for a global audience," in *Proc. MTS/IEEE Oceans Conf.*, Virginia Beach, VA, USA, Oct. 2012, pp. 1–5.

[4] X. Liu, X. Liu, T. Zhang, and Q. Wang, "Robust data cleaning methodology using online support vector regression for ultra-short baseline positioning system," *Rev. Sci. Instrum.*, vol. 90, no. 12, Dec. 2019, Art. no. 124901, doi: 10.1063/1.5078785.

[5] A. M. Sagalevich, "30 years experience of MIR submersibles for the ocean operations," *Deep Sea Res. II, Top. Stud. Oceanogr.*, vol. 155, pp. 83–95, Sep. 2018, doi: 10.1016/j.dsr2.2017.08.001.

[6] J. C. Kinsey, R. M. Eustice, and L. L. Whitcomb, "A survey of underwater vehicle navigation: Recent advances and new challenges," in *Proc. 7th Conf. Manoeuvering Control Mar.*, 2006, pp. 1–7.

[7] L. Medagoda, S. B. Williams, O. Pizarro, J. C. Kinsey, and M. V. Jakuba, "Mid-water current aided localization for autonomous underwater vehicles," *Auto. Robots*, vol. 40, no. 7, pp. 1207–1227, Oct. 2016, doi: 10.1007/s10514-016-9547-3.

[8] D. H. Titterton, and J. L. Weston, *Strapdown Inertial Navigation Technology*, 2nd ed. London, U.K.: Lavenham Press, Jan. 2004.

[9] P.-M. Lee and B.-H. Jun, "Pseudo long base line navigation algorithm for underwater vehicles with inertial sensors and two acoustic range measurements," *Ocean Eng.*, vol. 34, nos. 3–4, pp. 416–425, Mar. 2007, doi: 10.1016/j.oceaneng.2006.03.011.

[10] S. Arnold and L. Medagoda, "Robust model-aided inertial localization for autonomous underwater vehicles," in *Proc. IEEE Int. Conf. Robot. Autom. (ICRA)*, Brisbane, QLD, Australia, May 2018, pp. 4889–4896.

[11] Ø. Hegrenaes and O. Hallingstad, "Model-aided INS with sea current estimation for robust underwater navigation," *IEEE J. Ocean. Eng.*, vol. 36, no. 2, pp. 316–337, Apr. 2011, doi: 10.1109/joe.2010.2100470.

[12] Z. Song and K. Mohseni, "Long-term inertial navigation aided by dynamics of flow field features," *IEEE J. Ocean. Eng.*, vol. 43, no. 4, pp. 940–954, Oct. 2018, doi: 10.1109/JOE.2017.2766900.

[13] Y. Wu, X. Ta, R. Xiao, Y. Wei, D. An, and D. Li, "Survey of underwater robot positioning navigation," *Appl. Ocean Res.*, vol. 90, Sep. 2019, Art. no. 101845, doi: 10.1016/j.apor.2019.06.002.

[14] K. Tang, J. Wang, W. Li, and W. Wu, "A novel INS and Doppler sensors calibration method for long range underwater vehicle navigation," *Sensors*, vol. 13, no. 11, pp. 14583–14600, Oct. 2013, doi: 10.3390/s131114583.

[15] Y. Zhang, "An approach of DVL-aided SDINS alignment for in-motion vessel," *Optik*, vol. 124, no. 23, pp. 6270–6275, Dec. 2013, doi: 10.1016/j.ijleo.2013.05.010.

[16] B. Xu, L. Wang, S. Li, and J. Zhang, "A novel calibration method of SINS/DVL integration navigation system based on quaternion," *IEEE Sensors J.*, vol. 20, no. 16, pp. 9567–9580, Aug. 2020, doi: 10.1109/JSEN.2020.2988500.

[17] O. Hegrenaes, O. Hallingstad, and B. Jalving, "A framework for obtaining steady-state maneuvering characteristics of underwater vehicles using sea-trial data," in *Proc. Medit. Conf. Control Autom.*, Athens, Greece, Jun. 2007, pp. 1–6, doi: 10.1109/MED.2007.4433900.

[18] B. Sun, D. Zhu, and S. X. Yang, "A bioinspired filtered backstepping tracking control of 7000-m manned submarine vehicle," *IEEE Trans. Ind. Electron.*, vol. 61, no. 7, pp. 3682–3693, Jul. 2014, doi: 10.1109/TIE.2013.2267698.
[19] S. Zhang, J. Yu, A. Zhang, and F. Zhang, "Spiraling motion of underwater gliders: Modeling, analysis, and experimental results," *Ocean Eng.*, vol. 60, pp. 1–13, Mar. 2013, doi: 10.1016/j.oceaneng.2012.12.023.
[20] X. Liu, X. Liu, H. Shen, P. Li, and T. Zhang, "Self-aided SINS for spiral-diving human-occupied vehicle in midwater," *Assem. Autom.*, vol. 41, no. 1, pp. 106–115, Jan. 2021, doi: 10.1108/AA-05-2020-0072.
[21] Y. Yao, X. Xu, and X. Xu, "An IMM-aided ZUPT methodology for an INS/DVL integrated navigation system," *Sensors*, vol. 17, no. 9, p. 2030, Sep. 2017, doi: 10.3390/s17092030.
[22] X. Liu, X. Xu, Y. Liu, and L. Wang, "Kalman filter for cross-noise in the integration of SINS and DVL," *Math. Problems Eng.*, vol. 2014, Mar. 2014, Art. no. 260209, doi: 10.1155/2014/260209.
[23] J. Lu, Q. Luo, and Y. Yang, "Heave motion measurement by adaptive filter based on Longuet-Higgins wave model," *Math. Problems Eng.*, vol. 2017, Feb. 2017, Art. no. 6547312, doi: 10.1155/2017/6547312.
[24] G. Yan, X. Su, J. Weng, and Y. Qin, "Measurement of ship's heave motion based on INS and zero-phase-delay digital filter," *J. Navigat. Position*, vol. 4, no. 2, pp. 91–92, 2016, doi: 10.16547/j.cnki.10-1096.20160219.
[25] X. Liu, and X. Cheng, *Initial Alignment Theories and Methods for Strapdown Inertial Navigation System*. Beijing, China: Science Press, 2020.

XIANJUN LIU received the B.S. degree in automation from Harbin Engineering University, Harbin, Heilongjiang, China, in 2013. He is currently pursuing the Ph.D. degree in instrument science and technology with Southeast University, Nanjing, Jiangsu, China. His research interests include inertial navigation, integrated navigation, and information fusion, which applied in the field of underwater navigation technology.

XIXIANG LIU received the B.S. degree from Nanjing Forestry University, China, in 1999, and the M.S. and Ph.D. degrees from Southeast University, China, in 2004 and 2007, respectively.

From 2007 to 2010 and from 2010 to 2015, he was a Lecturer and an Associate Professor with Southeast University, China, where he has been a Professor, since 2015. His research interests include inertial sensors and navigation.

LEI WANG received the B.S. degree in optoelectronic information science and engineering from the Hefei University of Technology, Hefei, China, in 2008, and the Ph.D. degree in measuring and testing technologies and instruments from Zhejiang University, Hangzhou, China, in 2013.

He is currently working with Zhejiang University. His research interest includes the development of precise measurement of photoelectric sensors and underwater detection techniques.

YONGJIANG HUANG received the B.S. degree from Tiangong University, China, in 2013, and the M.S. degree from Southeast University, China, in 2017, where he is currently pursuing the degree. His research interests include inertial sensors and navigation.

ZIXUAN WANG was born in Jinan, Shandong, China, in 1998. He received the B.S. degree in mechanical design manufacture and automation from Shandong University, in 2020. He is currently pursuing the degree in electronic and communication with Southeast University. He has mainly researched on inertial navigation and integrated navigation. His research interests include integrated navigation and nonlinear optimization for information fusion.